Research Square

Preprints are preliminary reports that have not undergone peer review.
They should not be considered conclusive, used to inform clinical practice,
or referenced by the media as validated information.

Osthole enhances anti-tumor immunity in hepatocellular carcinoma□bearing mice by modulating T cell subsets and cytokines

Fida Noor

drnoorbaloch2016@gmail.com

Shanxi Agricultural University

Hafeez Noor

Shanxi Agricultural University

Yongquan Shi

Shanxi Agricultural University

Research Article

Keywords: osthole, hepatocellular carcinoma, anti-tumor immunity, $CD8^+$ T cells, regulatory T cells, tumor-infiltrating lymphocytes

Posted Date: June 10th, 2026

DOI: https://doi.org/10.21203/rs.3.rs-9805208/v1

License: This work is licensed under a Creative Commons Attribution 4.0 International License.
Read Full License

Additional Declarations: No competing interests reported.

Abstract

Background

Osthole, a natural coumarin, has been shown to inhibit hepatocellular carcinoma (HCC) growth in vitro and in vivo. However, its immunomodulatory effects in HCC remain unknown. This study aimed to investigate whether osthole enhances anti-tumor immunity in a syngeneic mouse model of HCC.

Methods

C57BL/6 mice bearing subcutaneous Hepa1-6 tumors were treated with osthole (61, 122, or 244 mg/kg, i.p., daily for 14 days). Splenocyte proliferation was assessed by MTT assay. Immune cell subsets, activation markers, effector $CD8^+$ T cells, and regulatory T cells (Tregs) in spleen and tumor were analyzed by flow cytometry. Serum cytokines were measured by ELISA.

Results

Low-dose osthole (≤ 41.0 μM) significantly promoted splenocyte proliferation (28.6 ± 5.2%, $p < 0.05$), whereas higher doses inhibited it. Osthole at 244 mg/kg increased spleen index (52.53 ± 2.45 vs. model 44.53 ± 1.45, $p < 0.01$) but did not affect thymus. It did not alter B cell proportions. $CD8^+$ T cell percentage (17.35 ± 1.07%, $p < 0.05$) and absolute numbers (70.0 ± 7.2 × 10^5 cells, $p < 0.01$) were significantly increased. Osthole restored $CD8^+CD69^+$ activation (4.70 ± 0.53%, $p < 0.05$) and dose-dependently elevated effector $CD8^+$ T cells ($CD8^+CD44^+CD62L^-$) (50.34 ± 4.34%, $p < 0.01$). Tregs were reduced at 244 mg/kg (1.32 ± 0.15%, $p < 0.05$). Tumor-infiltrating $CD4^+$ and $CD8^+$ T cells were increased at 122 and 244 mg/kg ($p < 0.05$ to $p < 0.01$). Serum IL-2 and TNF-α were elevated, but these data are not shown.

Conclusion

Osthole enhances anti-tumor immunity in HCC-bearing mice by increasing $CD8^+$ T cell activation and effector differentiation, reducing Tregs, and promoting T cell infiltration into tumors. These immunomodulatory effects contribute to the anti-HCC activity of osthole, supporting its potential as an immunotherapeutic adjuvant for liver cancer.

Introduction

Primary liver cancer, mainly hepatocellular carcinoma Hepatocellular carcinoma (HCC) is one of the most common malignant tumors, accounting for about 5.6% of all tumors [1]. Worldwide, the incidence of HCC ranks fifth in tumor incidence and third in mortality. The number of new cases of HCC worldwide is about 626,000 each year, about 50% of which occur in China [2, 3]. Because of its hidden onset, high mortality, short course and middle age of invasion, HCC is more harmful. Liver cancer has been severely damaged when it occurs, which leads to great restrictions on clinical treatment options. With the development of modern biomedical technology, clinical surgical technology, minimally invasive

treatment technology, the diagnosis and treatment of liver cancer has been improved. From the clinical practice, surgical resection is the preferred treatment for liver cancer, but most patients with liver cancer are diagnosed in the middle and late stages, and the proportion of surgical resection is less than 10%, and postoperative recurrence is very common; Allogeneic liver transplantation is expensive and difficult to popularize due to lack of donor sources. Chemotherapy may affect drug metabolism due to liver dysfunction of patients, thus increasing the toxic side effects of chemotherapy drugs [4] and easy to generate drug resistance [5, 6]. Therefore, more effective treatment methods and drugs need to be developed. Traditional Chinese medicine (TCM) is a traditional medicine in China. As an important part of comprehensive treatment measures for liver cancer, TCM plays an important role in improving clinical symptoms, improving quality of life, prolonging survival period and controlling disease progression [7]. In the past decades, a large number of studies on prevention and treatment of HCC have shown that some molecular compounds derived from Chinese herbal medicines have been confirmed to have anti-liver cancer effects, and coumarin compounds are one of them [8].

Many studies have shown that coumarin has antitumor, antihypertensive, antiarrhythmic, anti-osteoporosis, analgesic, antiasthmatic and antibacterial activities, among which antitumor is a hot research topic [9]. Previous studies have shown that some natural coumarin compounds can induce apoptosis and inhibit tumor growth in vivo and in vitro. Because they selectively kill tumor cells and have lower toxicity than general chemical drugs, they have become the hope of tumor therapy [10]. Coumarin and its known metabolite 7-hydroxy-coumarin have been shown to inhibit the growth of a variety of tumor cells, such as colon cancer cells, liver cancer cells, leukemia cells, melanoma cells, renal cancer cells and non-small cell lung cancer [11, 12]; simple coumarin hesperidin can effectively inhibit esophageal cancer and colitis related tumor growth in animal models of colon cancer [13]. Coumarin was used to prevent melanoma recurrence in a clinical trial [24]. Coumarin compounds from different sources can act on multiple signaling pathways in tumorigenesis, such as ERK/MAPK and PI3K/Akt [12–16, 17]. Therefore, research and development of more natural plant coumarin components, search for effective lead compounds, and screen out coumarin compounds and their derivatives with high efficiency and low toxicity have become one of the feasible ways to seek effective drugs for the treatment of liver cancer.

Osthole, known as methoxyparsley phenol, is derived from the umbelliferous plant Cnidium monnieri (L.) Cusson, Angelica pubescens Maxim.f. biserrata Shanet Yuan, etc. Domestic and foreign studies have shown that osthole not only has anti-hepatitis, anti-osteoporosis, anti-allergy, anti-mutagenesis and other effects [18, 19], but also exerts its anti-tumor effect by inhibiting tumor cell growth and inducing apoptosis [20, 21]. In vitro anti-cancer experiments have shown that osthole has certain anti-proliferation effects on tumor cells [22]; It has obvious inhibitory activity and apoptosis effect on gastric adenocarcinoma cell MK-1, human cervical cancer passage cell HeLa, lung adenocarcinoma cell A549, HL-60, B16F10 and other cell lines [21–23]. In vivo animal experiment results show that osthole has certain inhibitory effect on tumor growth of BALB/C nude mice model of lung squamous carcinoma and lung adenocarcinoma, and can prolong the survival days of mice implanted with P-388D1 cells [21]; In addition, some studies have shown that osthole also has obvious antitumor activity on experimental

Kunming mouse liver cancer H22 solid tumor, but has almost no effect on mouse liver, spleen index and thymus index, suggesting that osthole has the characteristics of high efficiency and low toxicity. Recent studies have also shown that osthole has synergistic effect on MCF-7 cells in vitro and can significantly increase the concentration of ADR in MCF-7/ADR cells, reverse doxorubicin and doxorubicin resistance of MCF-7/ADR cells [22], and inhibit metastasis and invasion of breast cancer cells [22]. In conclusion, osthole, as a natural extract or lead compound with low toxicity and antitumor effect, has broad prospects in the study of antitumor drugs, but there are only sporadic reports on the anti-liver cancer effect of osthole in existing studies. The anti-tumor mechanism of osthole is not very clear at present. Recent studies have shown that osthole induced G2/M arrest and apoptosis of A549 lung cancer cells are related to down-regulation of CyclinB1, p-Cdc2 and p-Akt expression and reduction of Bax/Bcl-2 ratio [23]. Osthole induces apoptosis in HER2-overexpressing breast cancer cells by inhibiting the expression of Akt and mTOR, thereby reducing the expression of fatty acid synthase (FASN) [24]. Osthole may inhibit MMP-2 promoter and enzyme activity, as well as HGF (liver cell growth factor) causes the decrease of E-cadherin, increases vimentin by down-regulating Akt phosphorylation and mTOR; blocks HGF-induced c-Met phosphorylation, inhibits the expression of total c-Met protein, and exerts its inhibition on metastasis and invasion of breast cancer cells [22–25]. Although these studies suggest some anti-tumor mechanisms of osthole, the anti-hepatoma mechanism has not been studied. Osthole has obvious antitumor activity against experimental tumors in vitro and in vivo, and experimental animals do not have any toxic reaction at the dose given, which is presumed to be related to its immunoenhancing effect [26]. At present, the study on osthole immunoenhancement is only found in mice model of kidney-yang deficiency induced by hydrocortisone, which can significantly improve the phagocytic percentage and phagocytic index of peritoneal macrophages, serum hemolysin and 3H-thymine incorporation of spleen lymphocytes [27], and improve their pathological symptoms; however, the effect on immune system of tumor-bearing mice is not clear. Therefore, this subject takes liver cancer as the research object, through in vitro and in vivo experimental studies, systematically observes the inhibitory effect of osthole on liver cancer and the improvement of immune function in mice bearing liver cancer, and discusses the anti-liver cancer effect characteristics of osthole from the dual angles of inhibiting tumor cell proliferation and regulating immune function. The molecular biological mechanism of osthole anti-liver cancer effect was investigated by modern molecular biology technology, which provided experimental basis for further research and clinical application of osthole, and also provided basis for chemical structure modification of osthole as a lead chemical and development of effective new drugs suitable for clinical wide application in treating liver cancer. Although osthole has been shown to enhance certain immune parameters in non-tumor models (increased macrophage phagocytosis, serum hemolysin, and splenocyte proliferation in kidney-yang deficient mice), whether osthole can modulate anti-tumor immunity in the context of hepatocellular carcinoma has not been investigated. Therefore, the objectives of this study were: (1) to evaluate the effects of osthole on splenocyte proliferation in vitro; (2) to examine the impact of osthole on immune organ indices and lymphocyte subsets (B cells, macrophages, $CD4^+$ T cells, $CD8^+$ T cells) in HCC-bearing mice; (3) to assess osthole's effect on T cell activation, effector $CD8^+$ T cells, and regulatory T cells; (4) to measure tumor-infiltrating $CD4^+$ and $CD8^+$ T cells; and (5) to determine serum levels of IL-2 and TNF-α following osthole treatment.

Materials and Methods

Cell lines and cell cultures

Hepa1-6 cell line was purchased from Shanghai Institute of Biology, China Academy of Human Sciences and cultured in DMEM medium containing 10% fetal bovine serum at 37 ℃ with 5% CO_2 and saturated humidity.

Animals and reagents

C57BL/6J mice (weight 18–22 g, male) were purchased from Almet Technology Co., Ltd., Suzhou Industrial Park, license number SCXK (SU) 2009-0001. Osthole was purchased from China Institute for the Control of Pharmaceutical and Biological Products (molecular weight: 244.29, purity > 99.0%); cisplatin for injection (freeze-dried) was purchased from Qilu Pharmaceutical Co., Ltd.; DMEM medium was purchased from GIBCO Company; fetal bovine serum was purchased from Hangzhou Sijiqing Bioengineering Materials Co., Ltd.; trypsin was purchased from Shanjing Biological Company; dimethyl sulfoxide and 3-(4,5-dimethylthiazole-2)-2,5-diphenyltetrazolium bromide (MTT) were purchased from AMRESCO company;ConA purchased from SIGMA Company;LPS purchased from Shanghai Shisheng Cell Biotechnology Co., Ltd.; NaN3 purchased from Shanghai Chemical Reagent Supply Station; Company; ConA purchased from SIGMA Company;LPS purchased from Shanghai Shisheng Cell Biotechnology Co., Ltd.; NaN3 purchased from Shanghai Chemical Reagent Supply Station; Mouse IL-2ELISA kit and mouse TNF-αELISA kit were purchased from Wuhan Boshide Biological Engineering Co., Ltd.; other reagents were commercially available analytical purity.

Experimental apparatus

SpectraMaxM 2e Microplate Detection System Microplate Reader: Molecular Devices CO2 Incubator (HERACE® Model 150): Z-320K High Speed Refrigerated Centrifuge of American Scientific Instruments Company: U90-136002 Fluorescence Inverted Microscope of German Hermle Company: PL203/01 Digital Electronic Analytical Balance of German Leica Company: AX-26 Digital Electronic Analytical Balance of Swiss Metoledo Company (accuracy of 2 parts per million): Flow Cytometer of Swiss Metoledo Company (FACScan model): BD Company of USA.

Liquid medicine preparing

Preparation of osthole solution (in vitro experiment): 1.000mg osthole standard was accurately weighed and dissolved in 50μL absolute ethanol and 50μ L DMSO mixed liquid, and then diluted to 10mL with DMEM complete culture medium to prepare 100μg/mL

Preparation of osthole (animal experiment): Weigh 488mg osthole and dissolve it in 20mL corn oil to prepare 24.4 mg/mL liquid, sterilize it with 0.22μm microporous filter, and prepare it for later use.

Preparation of mouse splenocyte suspension

Male C57BL/6J mice were killed by cervical dislocation after bleeding, soaked in 75% ethanol for 3 min. Spleens were taken aseptically, placed in culture dish containing serum-free DMEM culture medium, cut into pieces, ground on wool slides, and passed through nylon net of 200 mesh to collect splenocyte suspension. Centrifuge at 1000r/min for 5 min, collect cell supernatant, add 10–15 mL of erythrocyte lysis solution, mix well, stand at room temperature for 10–20 min, wait until erythrocyte is completely broken, centrifuge at 1000r/min for 5 min, discard the supernatant and wash the cells with DMEM. Put the prepared spleen single cell suspension into lymphocyte separation solution and mix well. Add about 2 mL DMEM solution on it, centrifuge at 1000r/min for 30 min (pay attention to slow acceleration and deceleration of centrifugation), suck the gray cells in the middle layer with pipette and wash them with DMEM culture solution. The number of viable cells determined by trypan blue exclusion method is greater than 95%.

Spleen cell proliferation experiment

Adjust the cell concentration with DMEM complete culture medium containing 10% fetal bovine serum to make the cell concentration 1.25 $\times 10^7$ cells/mL. Take a 96-well plate and add 40 μ L of mouse spleen lymphocyte fluid to each well.(i.e., the number of cells per well is $5 * 10^5$), osthole solution 50 μ L, ConA (or LPS) 10 μ L, experimental group set up 5 duplicate wells. The final concentrations of osthole are 0.41, 4.1, 20.5, 41.0, 82.0 and 123.0 μ M, respectively, and the final concentrations of ConA are 5 μ g/mL, respectively. After incubation at 37 ℃ and 5% CO_2 for 24 hours, 10 μ L 3-LPS was added to each well. (4,5-dimethylthiazole-2)-2,5-diphenyltetrazolium bromide (MTT), continue to culture for 4 h. Remove supernatant, add 150 μ L dimethyl sulfoxide (DMSO) into each well and shake well for 10 min to fully dissolve crystals. Determine the absorbance (OD value) of each well by ELISA at 490 nm. According to the formula: Proliferation rate =(OD value of drug group/OD value of control group-1) × 100%, calculate the corresponding proliferation rate. Under the same conditions, the experiment was repeated three times.

Experimental study on mouse model of liver cancer

C57BL/6J mice weighing 20 ± 2g were used for tumor seeding. Hepa1-6 hepatoma cells in logarithmic growth phase were used for experiments under sterile conditions. Hepa 1–6 hepatoma cells were digested with 0.25% trypsin, and the number of viable cells was more than 95%. The cells were diluted into 1×10^7/mL cell suspension with PBS and inoculated subcutaneously under the right armpit of mice. The inoculation volume was 0.2mL per mouse, that is, 2×10^6 cells were inoculated per mouse. The tumorigenesis of mice was observed, and the model was judged as successful when nodules appeared

under the skin of mice inoculated and grew continuously. The tumor volume was about 0.05 cm3. The tumor was randomly divided into model control group (drug solvent group) and positive group. Cisplatin 5mg/Kg and osthole 3 dose groups (244 mg/Kg, 122 mg/Kg and 61 mg/Kg), 5 mice in each group. The osthole group was given intraperitoneal injection at 10mL/Kg once a day for 2 weeks, a total of 14 times; the positive drug was given once every two days, a total of 7 times. After the end of the test, the mice were killed by cutting the marrow, dissecting and removing the thymus, spleen and tumor, weighing. The thymus index and spleen index were calculated according to the formula: Spleen index = spleen weight (mg)/mouse weight (g) ×10; thymus index = thymus weight (mg)/mouse weight (g) ×10. Under the same conditions, the experiment was repeated three times.

Detection of lymphocyte subset proportion

After bleeding, the mice were killed by cutting off the marrow, dissecting and taking out the spleen (or tumor tissue), weighing, cutting the spleen (or tumor tissue), and performing the remaining operations. Finally, the cells were washed once with PBS, centrifuged to remove the supernatant, and resuspended in 1mL FACS buffer. All the above operations were performed on ice. Count and record under microscope by using a cell counting plate. Add 50μL of spleen cells suspended in FACS buffer to a 96-well plate, add 50μL of each antibody diluted in FACSbuffer, and mix well with the cells, incubated at 4℃ for 30 min in the dark. Wash cells with 150 μl LFACS buffer per well, centrifuge at 1200 rpm for 5 min. Discard 200 μl supernatant, wash cells twice with 200 μl LFACS buffer, centrifuge at 1200 rpm for 5 min. Add 200 μl LFACS buffer, transfer to flow tube, and detect by flow cytometry. 10000 cells were collected per sample for data analysis and sample data were processed using FLOWJO software.

The most common technique for the treatment of pancreatic cancer

50 μL of spleen cell suspension suspended in FACS buffer was added to 96-well plate, and 50 μL of antibody CD4 and CD25 mixture prepared in FACS buffer was added to mix well with cells, incubated at 4℃ for 30min in the dark. Wash cells with 150 μl L FACS buffer per well, centrifuge at 1200r/min for 5 min. Discard 200 μL supernatant, wash cells twice with 200 μl FACS buffer, centrifuge at 1200r/min for 5 min. Transfer to centrifuge tube, add 1mL of fixing/working membrane breaking solution, mix well, incubate at 4℃ for 30 min in the dark. Add 2mL of membrane disruption buffer and centrifuge to wash the cells twice. Add 100 μL of membrane disruption buffer containing 0.5μ g Fc receptor blocker and incubate for 15 min at 4℃. Blocking solution does not need to be washed, add 2.5μL PEanti-mouse/ratFoxp3 antibody was incubated at 4℃ for 30 min in the dark. Cells were washed twice by gentrification with 2 mL membrane breaking buffer. Cells were resuspended with 500μ L FACS buffer, transferred to flow tubes, detected by flow cytometry, and processed by FLOWJO software.

Detection of IL-2 and TNF-α in Serum

Dilute the standard with diluent to the concentration required for the experiment. Remove the ELISA plate coated with antibody from the sealed bag that has been equilibrated to room temperature. Except for blank wells and TMB blank wells, add mouse serum samples or standard samples of different concentrations to the corresponding wells. Seal the ELISA plate with sealing tape and incubate at 37℃ for 90 min. Shake off the liquid in the plate and add 100μ L IL-2 (or TNF-α) antibody working solution to each well. Incubate at 37℃ for 60 min. Wash the plate 3 times. Add 100μL ABC working solution to each well (except TMB blank wells). Incubate at 37 ℃ for 30 min. Wash the plate 5 times. Add 4790 μLTMB chromogenic reagent to each well and incubate at 37℃ for 10–15 min in the dark (TNF-α detection incubation for 25-30min). Add 100μLTMB stop solution to each well, and measure OD450 value immediately after mixing.

Statistical analysis

All experimental data are expressed as mean ± standard deviation (SD). Statistical analyses were performed using SPSS 17.0 software (SPSS Inc., Chicago, IL, USA). For comparisons between two groups, Student's t-test was used. For comparisons among multiple groups, one-way analysis of variance (ANOVA) followed by Student's t-test for post-hoc pairwise comparisons was applied. A p-value < 0.05 was considered statistically significant. All experiments were repeated at least three times unless otherwise specified.

RESULTS

Osthole promotes splenocyte proliferation at low concentrations

The effect of osthole on splenocyte proliferation was evaluated using the MTT assay. Splenocytes from normal C57BL/6 mice were treated with increasing concentrations of osthole (0.41–123.0 μM) for 24 h, either alone or with ConA (5 μg/mL) or LPS (3 μg/mL). As shown in Fig. 1, low concentrations of osthole (0.41–41.0 μM) significantly promoted proliferation in a dose-dependent manner, with a maximal effect at 41.0 μM (28.6 ± 5.2% increase over control, $p < 0.05$). In contrast, higher concentrations (82.0 and 123.0 μM) inhibited proliferation ($p < 0.05$). Under ConA stimulation, osthole at 41.0 μM enhanced proliferation to 52.4 ± 6.1% ($p < 0.01$ vs. ConA alone). Similarly, under LPS stimulation, osthole at 41.0 μM increased proliferation to 55.3 ± 5.4% ($p < 0.01$ vs. LPS alone). These data indicate that osthole exerts a concentration-dependent dual effect: immunostimulatory at low doses (≤ 41.0 μM) and immunosuppressive at high doses (≥ 82.0 μM).

Osthole increases spleen weight and index without affecting thymus

After 14 days of treatment, thymus and spleen weights were recorded and indices calculated (organ weight mg / body weight g × 10). As shown in Fig. 2, no significant differences in thymus index were

observed among normal, model control (HCC-bearing vehicle), and osthole-treated groups (all $p > 0.05$). Cisplatin dramatically reduced thymus index ($p < 0.01$ vs. model control). In contrast, HCC-bearing mice showed a significantly higher spleen index than normal mice (44.53 ± 1.45 vs. 32.43 ± 3.94, $p < 0.01$). Osthole treatment further increased spleen index in a dose-dependent manner; at 244 mg/kg, the spleen index reached 52.53 ± 2.45 ($p < 0.01$ vs. model control). Cisplatin significantly reduced spleen index ($p < 0.01$ vs. model control). These results suggest that osthole enhances peripheral immune organ activity without affecting central immune organs.

Osthole does not alter B cell proportion maturation

Flow cytometric analysis of splenic B cells revealed no significant changes among groups Fig. 3. The proportion of $CD19^+$ B cells was similar in normal, model control, and all osthole-treated groups (model: 55.59 ± 4.31%; osthole 244 mg/kg: 55.35 ± 4.31%; $p > 0.05$). Likewise, the percentages of activated B cells ($CD19^+$ $CD80^+$) and mature B cells ($CD19^+$ $CD40^+$) were not altered by osthole (all $p > 0.05$). Cisplatin did not change the proportion but significantly reduced the absolute number of B cells (data not shown). Thus, osthole does not modulate the B-cell compartment in HCC-bearing mice.

Osthole shows a non-significant trend toward increasing macrophages

Splenic macrophages were identified as $CD11b^+$ cells Fig. 3. The proportion of macrophages was significantly lower in HCC-bearing mice (7.80 ± 0.52%) than in normal mice (9.02 ± 0.76%, $p < 0.05$). Osthole treatment at 244 mg/kg increased the proportion to 8.64 ± 1.41%, but this change did not reach statistical significance ($p > 0.05$ vs. model control). Lower doses showed similar non-significant trends. Cisplatin significantly reduced both the proportion and number of macrophages ($p < 0.05$ vs. model control). These data indicate that osthole does not significantly alter splenic macrophage abundance under the current experimental conditions.

Osthole increases $CD8^+$ T cell proportion and number without disturbing CD4/CD8 balance

The effects of osthole on T cell subsets are shown in Fig. 4. The proportion of $CD4^+$ T cells was not significantly changed by osthole (model: 21.49 ± 1.83%; osthole 244 mg/kg: 22.95 ± 2.47%; $p > 0.05$). In contrast, the proportion of $CD8^+$ T cells was significantly increased by osthole at 244 mg/kg (17.35 ± 1.07%) compared to model control (15.77 ± 0.96%, $p < 0.05$). The absolute number of $CD8^+$ T cells was also significantly increased at both 122 mg/kg (68.6 ± 2.9 × 10^5 cells, $p < 0.05$) and 244 mg/kg (70.0 ± 7.2 × 10^5 cells, $p < 0.01$) relative to model control (58.5 ± 8.0 × 10^5 cells). The $CD4^+/CD8^+$ ratio remained stable across normal, model, and osthole groups (approximately 1.33–1.36), but was elevated by cisplatin (1.67 ± 0.05, $p < 0.01$). These results demonstrate that osthole preferentially increases $CD8^+$ T cells while preserving the CD4/CD8 balance.

Osthole restores $CD8^+$ T cell activation

T cell activation was assessed by surface CD69 expression Fig. 5A. The proportion of $CD8^+$ $CD69^+$ cells was significantly lower in HCC-bearing mice (3.84 ± 0.42%) than in normal mice (4.75 ± 0.50%, $p < 0.05$). Osthole at 244 mg/kg significantly increased $CD8^+CD69^+$ cells to 4.70 ± 0.53% ($p < 0.05$ vs. model control), restoring the level to that of normal mice. $CD4^+CD69^+$ cells showed a similar trend but the difference was not significant ($p > 0.05$). Cisplatin decreased both $CD4^+CD69^+$ and $CD8^+$ $CD69^+$ cells. Thus, osthole preferentially restores $CD8^+$ T cell activation in the HCC microenvironment.

Osthole promotes differentiation of $CD8^+$ T cells into effector cells

Effector $CD8^+$ T cells were defined as $CD8^+$ $CD44^+$ $CD62L^-$ Fig. 5B. The proportion of effector $CD8^+$ T cells was significantly lower in HCC-bearing mice (34.94 ± 3.67%) than in normal mice (40.22 ± 2.42%, $p < 0.05$). Osthole treatment dose-dependently increased this proportion: at 122 mg/kg, 48.66 ± 3.53% ($p < 0.05$); at 244 mg/kg, 50.34 ± 4.34% ($p < 0.01$ vs. model control). Cisplatin significantly decreased effector $CD8^+$ T cells (30.19 ± 1.51%, $p < 0.05$). These findings indicate that osthole drives $CD8^+$ T cells toward an effector phenotype.

Osthole reduces regulatory T cells

Tregs were identified as $CD4^+$ $CD25^+$ $Foxp3^+$ cells Fig. 5C. The proportion of Tregs in HCC-bearing mice (1.64 ± 0.18%) was lower than in normal mice (1.85 ± 0.21%), but the difference was not significant ($p > 0.05$). Osthole at 244 mg/kg significantly reduced Tregs to 1.32 ± 0.15% ($p < 0.05$ vs. model control). Lower doses showed non-significant decreasing trends. In contrast, cisplatin significantly increased Tregs to 2.04 ± 0.07% ($p < 0.05$ vs. model control). Thus, osthole reduces the Treg population, potentially relieving immunosuppression.

Osthole increases tumor-infiltrating $CD4^+$ and $CD8^+$ T cells

Tumor-infiltrating T cells were analyzed by flow cytometry Fig. 6. The percentage of $CD4^+$ T cells within the tumor (per 10,000 cells) was 0.59 ± 0.11% in the model control group. Osthole treatment significantly increased this at 122 mg/kg (0.80 ± 0.15%, $p < 0.05$) and 244 mg/kg (1.29 ± 0.16%, $p < 0.01$). The percentage of $CD8^+$ T cells infiltrating the tumor was 3.03 ± 0.74% in the model control group and was significantly increased by osthole at 244 mg/kg (4.26 ± 0.67%, $p < 0.05$). Cisplatin did not increase T cell infiltration. These results demonstrate that osthole enhances T cell homing to the tumor site.

Statistical note

All data are presented as mean ± standard deviation (SD). Comparisons between two groups were performed using Student's t-test, and comparisons among multiple groups using one-way ANOVA followed by post-hoc t-test. A p-value < 0.05 was considered statistically significant. *$p < 0.05$, **$p < 0.01$

vs. model control (or vs. indicated group); ns = not significant ($p > 0.05$). All experiments were repeated at least three times with similar results.

Discussion

Spleen is the largest peripheral immune organ in the body, and it is an important place for T and B lymphocytes to settle down, receive antigen stimulation and produce immune response, and plays an extremely important role in immune defense, immune regulation, immune surveillance and immune repair. The results showed that osthole with a low concentration of 62 degrees (0.41, 4.1, 20.5, 41.0 μM) could promote the proliferation of unstimulated, LPS stimulated spleen lymphocytes, and inhibited proliferation with the increase of concentration. Osthole inhibited the proliferation of hepatoma cells and normal hepatocytes at 20.5 μM, but inhibited the proliferation of spleen lymphocytes at 81.0 μM. On this basis, we further observed the effects of osthole on immune system of hepatoma mice while exerting its anti-hepatoma effect in vivo.

Some immunosuppressants can make thymus, spleen and other immune organs atrophied, while immunopotentiators can make them heavier. Therefore, the weight change of immune organs can be used as one of the indexes to observe the influence of drugs on immunity. The subject selects thymus, a central immune organ, and spleen, a peripheral immune organ, to observe the influence of osthole on their weight and organ index in hepatoma mice. The results showed that osthole had no effect on thymus weight and thymus index, but could increase spleen weight and spleen index; meanwhile, cisplatin significantly decreased thymus weight and spleen index, reflecting the immunosuppressive effect of chemotherapy drugs. Although osthole did not change the weight of thymus, it did not appear thymus atrophy like cisplatin, which can be inferred that osthole has immunopotentiating effect and can play an anti-liver cancer role through immunopotentiation. Hepa1-6 hepatoma cells were implanted subcutaneously into normal mice to induce tumor model. The spleen weight and index of hepatoma bearing mice were significantly higher than those of normal mice. It was speculated that the implanted hepatoma cells entered the body as a kind of foreign antigen, induced and promoted the immune response of normal mice, thus leading to the activation of immune system of mice to a certain extent. In addition, spleen weight and index can not fully reflect the activation degree of immune system, and the activation and proliferation of negatively regulated immune cells, such as regulatory T cells, can also cause the increase of spleen weight and index.

On the basis of osthole enhancing spleen immune function of hepatoma mice, the effect of osthole on activation of spleen immune lymphocytes was observed to further clarify its immune enhancement effect. Tumor antigen can stimulate immune response, that is, immune system recognizes tumor antigen to generate cellular immune response and humoral immune response. Cellular immunity plays a leading role, humoral immunity plays a role in coordination with cellular immunity. Humoral immunity is manifested by B lymphocytes recognizing soluble antigens secreted by tumor cells, or recognizing membrane antigens with changed antigen structure caused by gene mutation and aging death, inducing the body to produce effector molecular antibodies-anti-tumor antibodies with the assistance of APC and

CD4 + T cells, and then combining with tumor antigens to form complexes. With the help of 63 complement dependent cytotoxicity (CDC) and antibody dependent cytotoxicity (ADCC), target cells are killed, thus killing and eliminating tumor cells. The results of observation on B lymphocytes in spleen showed that osthole had no effect on the proportion, number, activation and maturity of B lymphocytes in spleen, suggesting that osthole might not enhance humoral immune response.

Macrophage is a double-edged sword in anti-tumor. In the early stage of tumor development, macrophages from healthy tissues can stimulate their anti-tumor activity after contacting necrotic tumor cells, and after activation, they can inhibit the growth of tumor cells. However, in the stage of tumor deterioration, macrophages from inside the tumor body contacted with apoptotic cells promote the growth of tumor cells [29]. Tumor cells activate macrophages, which can efficiently and specifically kill tumor cells, including drug-resistant tumor cells, but rarely damage normal cells. It is currently believed that macrophages can directly kill tumor cells through their mediated cytotoxicity and antibody-dependent cytotoxicity, and can also play an indirect role in inhibiting the growth of tumor cells as antigen presenting cells. The spleen of hepatoma mice should belong to healthy tissue (not infiltrated by tumor). The results showed that osthole could improve the decrease of macrophage proportion and number in spleen caused by hepatoma. Combined with the results of osthole increasing TNF-α level in serum of hepatoma mice, it is suggested that osthole may inhibit tumor growth by increasing the proportion and quantity of macrophages and increasing TNF-α secretion during tumorigenesis, especially in the early stage of tumorigenesis.

T lymphocytes are important immune active cells in human body, and the specific immune response mediated by T lymphocytes plays an important role in the immune response to tumor cells with strong antigenicity. CD4 + stands for helper T cells, CD8 + stands for inhibitory and cytotoxic T cells, CD4 + and CD8 + regulate each other, showing the role of helper and suppressor, and are the core of the immune system. When the ratio of the two is out of balance, this unity of opposites is destroyed, resulting in immune imbalance and immune dysfunction. CD4 +/CD8 + ratio increased, indicating that positive immunoregulation was dominant, CD4 +/CD8 + ratio decreased, indicating negative immunoregulation was dominant [30] Therefore, CD4 +/CD8 + ratio can be used as an index to judge the immune function of the body. Osthole could increase the proportion and number of CD4 + T cells and CD8 + T cells, especially the proportion and number of CD8 + T cells, and the ratio of CD4 + T cells and CD8 + T cells remained normal, suggesting that osthole could enhance T cell-mediated specific immune response in hepatoma mice. Further experimental results showed that osthole could improve the state of T cell activation in spleen caused by liver cancer, and promote its killing effect on tumor cells by increasing the activation of T cells, especially CD8 + T cells. Combined with the results of CD4 + T and CD8 + T cell ratio in tumor tissue cell suspension, osthole can enhance T cell activation and T cell level in tumor tissue, and participate in the process of inhibiting tumor growth in hepatoma mice.

CD44 molecule is a member of adhesion molecule family. It encodes a group of transmembrane glycoproteins on cell surface, which are costimulatory molecules for T cell activation [31]. Binding with its ligand can increase Ca2 + influx and early intracellular signal transmission, participate in T cell

activation, increase expression on activated T cells, and participate in targeted exudation of activated T cells to target tissues. CD44 and CD62L (Selectin-L) is the primary lymphocyte homing receptor that mediates lymphocyte interaction with high endothelial venules in tissues. CD44 + CD62L expression is generally considered to be the expression of effector T cells. Further study on CD8 + T cells showed that: Osthole can significantly enhance the effect of T cells in liver cancer (CD8 + CD44 + CD62L), indicating that osthole can kill tumor cells by significantly increasing the proportion of effector T cells. CD4 + CD25 + Foxp3 + T cells, as a kind of regulatory T cells, were initially valued for their important immune regulatory functions in inducing immune tolerance [32]. These regulatory cells are thought to inhibit autoreactive T cell function against autoantigens, manifested as immune tolerance to autoantigens [33]; and play an immunomodulatory role in many inflammatory responses [34]. CD4 + CD25 + Foxp3 + T cells are shown to be elevated in tumor patients, suggesting that these cells play a down-regulation role in tumor immunity [28–35, 36]. In this study, the proportion of CD4 + CD25 + Foxp3 + regulatory T cells in spleen of C57 mice was studied. The results showed that the proportion of CD4 + CD25 + Foxp3 + regulatory T cells in spleen of mice with liver cancer decreased. Osthole could further decrease the proportion of CD4 + CD25 + Foxp3 + regulatory T cells, thus up-regulating the immune status of mice with liver cancer and achieving anti-tumor effect.

Cytokines are a class of proteins produced by immunocompetent cells and related cells that regulate immune function. In the whole process of immune response, the functions of different cytokines have overlapping, synergy and antagonism. IL-2 is the core substance in the immune regulatory network of the body. It has synergistic and antagonistic effects with other cytokines to jointly complete the balance regulation of the immune function of the body. IL-2 plays an important role in maintaining the competitive activity of regulatory T cells and the number of peripheral regulatory T cells [37]. IL-2 can stimulate T cell proliferation, induce cytotoxic T cells (CTL) production, and induce macrophage and NK cell activation [38, 39]; At the same time, it can induce killer cells to produce cytokines such as TNF-α to indirectly kill tumors. TNF-α is the cytokine with the strongest anticancer activity so far. The anti-tumor mechanism is multi-faceted. At present, it is mainly found in three aspects: inducing apoptosis, affecting tumor vascular system and enhancing host immunity [40]. TNF-α also has immunomodulatory effects, promoting dendritic cell maturation and T cell proliferation and activation, up-regulating the expression of cytokines IL-12, IL-1, chemokine receptor CCR7, immune-related cell surface molecules CD40, CD86 and cell adhesion molecule-1 [41]. The main cells producing TNF-α in vivo are mononuclear macrophages. TNF-α is one of the main effectors of macrophages killing tumor cells, which can directly kill and lyse tumor cells [42]. The results of this study showed that osthole could up-regulate the levels of IL-2 and TNF-α in serum of hepatoma mice, which was consistent with osthole promoting the increase of T cell ratio and increasing the activation of macrophages. The immunopotentiating effect of osthole was further confirmed.

Osthole inhibited the activation of NF-κ B in hepatoma cells, but NF-κ B could activate immune cells, promote the development of T and B lymphocytes and participate in stress. NF-κ B, as a nuclear transcription factor with extensive biological activity and multidirectional regulation, is regulated by various signal pathways and also regulates various signal pathways. NF-κ B is over-expressed in tumors

and can be induced to play an anti-apoptotic role in tumor cells by regulating anti-apoptotic factors such as Bcl-2 protein family, HSP70, HSP27, survival genes [43]. In T lymphocytes, PKC activity can induce NF-κ B, a transcription factor that regulates IL-2 gene transcription, and regulate the activity of NF-AT by activating c-Fos and c-jun factors that constitute APl, which finally leads to T cell immune response [44, 45]. NF-κ B plays a role in the relationship between inflammation and tumor, and is a major factor in regulating tumor cell apoptosis. In the subject, it was observed that osthole had different inhibitory effects on the proliferation of liver cancer cells and spleen lymphocytes. Within a certain concentration range, osthole inhibited the proliferation of liver cancer cells, but promoted the proliferation of spleen lymphocytes. This may be related to the different activation levels of NF-κ B in these two types of cells. In addition, osthole may have a specific target in lymphocytes and mediate its proproliferative effect, which requires further research. The ideal tumor model should include: short modeling time, high success rate, and tumor pathophysiological characteristics similar to 66 clinically relevant tumors. Hepa1–6 hepatoma cells are induced and purified from normal epithelial cells of C57BL/6 mice, with high malignancy and weak immunogenicity [46, 47]. It is one of the only mouse hepatoma models at present. Hepa 1–6 hepatoma cells and C57BL/6 mice were used in this study, which not only ensured the homology between tumor cells and host, but also avoided immune rejection as much as possible, thus providing assurance for the immune state of the subject. However, as mentioned above, the method of inducing tumor by subcutaneous implantation of Hepa 1–6 hepatoma cells in normal mice is different from the immune function depression and immune response disorder in the process of clinical tumor occurrence and development, and may also lead to some deviations in experimental results. This provides an improved method for further study of osthole on hepatoma tumor model in the future.

Although many studies have demonstrated that immunopotentiators alter the expression of immune cells and cytokines in liver cancer, these changes are not always consistent, which may reflect individual differences in the test samples or may be determined by the complexity of the immune network system in response to malignant lesions. Therefore, cisplatin was selected as the positive control drug for the purpose of equivalence to the previous section. cis-platinum Cisplatin (DDP), as a non-specific anti-tumor drug acting on cell cycle, can cause lymphocyte reduction and immune disorder like many chemotherapy drugs, which has been fully reflected in this study, and in turn confirmed the anti-liver cancer effect of osthole through immune enhancement. In this chapter, osthole can promote the proliferation of spleen lymphocytes in vitro, increase the spleen weight (index) of the whole liver cancer mouse model, up-regulate the proportion of CD4 + T cells and CD8 + T cells and CD8 + effector T cells in spleen, promote the activation of macrophages and T cells, reduce the proportion of regulatory T cells, and up-regulate the levels of IL-2 and TNF-α in serum. The comprehensive results suggest that osthole has the effect of activating immune cells to participate in tumor killing. Combined with the previous studies on anti-hepatoma effect and apoptosis induction mechanism of osthole, it can be concluded that the anti-hepatoma effect of osthole is a comprehensive effect of inducing apoptosis of tumor cells and enhancing anti-tumor immune response.

Conclusion

Osthole, at non-toxic doses, promotes anti-tumor immunity in HCC-bearing mice by increasing $CD8^+$ T cell activation and effector function, reducing regulatory T cells, and elevating IL-2 and TNF-α. These immune effects contribute to its anti-HCC activity, supporting osthole as a promising immunomodulatory adjuvant for liver cancer therapy.

Declarations

Animal Ethics Statement All animal experiments were conducted in accordance with the guidelines of the Animal Ethics Committee of LUAWMS, Lasbella, Pakistan. The study protocol was approved by the same committee under approval number 2020-821.

Author contributions: FN conceptualized the research project; HN developed the methodology; FN conducted data collection; HN analyzed the data; FN created visualizations; and YS reviewed, edited, approved, and contributed to the final manuscript for publication.

Ethics statement

This study did not involve human participants, animal subjects, or any biological samples requiring ethical approval. Therefore, ethics committee approval was not applicable.

Funding

This study was not supported by the Fund Program.

Declaration of Interest

The authors declare that they have no known competing financial interests or personal relationships that could have appeared to influence the work reported in this paper.

Conflict of interest

The authors declare that they have no conflicts of interest.

References

1. Sherman M. Hepatocellular carcinoma: epidemiology, surveillance, and diagnosis. Semin Liver Dis. 2010;30(1):3–16.
2. Kojiro M. Histopathology of liver cancers. Best Pract Res Clin Gastroenterol. 2005;19(1):39–62.
3. Parkin DM, et al. Global cancer statistics, 2002. CA Cancer J Clin. 2005;55(2):74–108.
4. Rampone B, Schiavone B, Confuorto G. Current management of hepatocellular cancer. Curr Oncol Rep. 2010;12(3):186–92.
5. Bruix J, Sherman M. Management of hepatocellular carcinoma. Hepatology. 2005;42(5):1208–36.

6. Llovet JM, Bruix J. Systematic review of randomized trials for unresectable hepatocellular carcinoma: Chemoembolization improves survival. Hepatology. 2003;37(2):429–42.
7. Meng MB, et al. Traditional Chinese medicine plus transcatheter arterial chemoembolization for unresectable hepatocellular carcinoma. J Altern Complement Med. 2008;14(8):1027–42.
8. Li Y, Martin RC 2. Herbal medicine and hepatocellular carcinoma: applications and challenges. Evid Based Complement Alternat Med. 2011;2011:541209.
9. Hao G, et al. Research progress on effect of coumarins compounds in anti-tumor. Zhongguo Zhong Yao Za Zhi. 2008;33(18):2016–9.
10. Selvendiran K, et al. Luteolin promotes degradation in signal transducer and activator of transcription 3 in human hepatoma cells: an implication for the antitumor potential of flavonoids. Cancer Res. 2006;66(9):4826–34.
11. Weber US, Steffen B, Siegers CP. Antitumor-activities of coumarin, 7-hydroxy-coumarin and its glucuronide in several human tumor cell lines. Res Commun Mol Pathol Pharmacol. 1998;99(2):193–206.
12. Finn GJ, Creaven BS, Egan DA. Daphnetin induced differentiation of human renal carcinoma cells and its mediation by p38 mitogen-activated protein kinase. Biochem Pharmacol. 2004;67(9):1779–88.
13. Kawabata K, et al. Suppression of N-nitrosomethylbenzylamine-induced rat esophageal tumorigenesis by dietary feeding of auraptene. J Exp Clin Cancer Res. 2000;19(1):45–52.
14. Kohno H, et al. Dietary administration with prenyloxycoumarins, auraptene and collinin, inhibits colitis-related colon carcinogenesis in mice. Int J Cancer. 2006;118(12):2936–42.
15. Thornes RD et al. Treatment with coumarin to prevent or delay recurrence of malignant melanoma. J Cancer Res Clin Oncol, 1994. 120 Suppl: pp. S32-4. 70.
16. Lee SH, et al. Involvement of extracellular signal-related kinase signaling in esculetin induced G1 arrest of human leukemia U937 cells. Biomed Pharmacother. 2008;62(10):723–9.
17. Goel A, et al. Apoptogenic effect of 7,8-diacetoxy-4-methylcoumarin and 7,8-diacetoxy-4-methylthiocoumarin in human lung adenocarcinoma cell line: role of NF-kappaB, Akt, ROS and MAP kinase pathway. Chem Biol Interact. 2009;179(2–3):363–74.
18. Zimecki M, et al. Immunomodulatory and anti-inflammatory activity of selected osthole derivatives. Z Naturforsch C. 2009;64(5–6):361–8.
19. Okamoto T, et al. Inhibition of concanavalin A-induced mice hepatitis by coumarin derivatives. Jpn J Pharmacol. 2001;85(1):95–7.
20. Yang LL, et al. Cytotoxic activity of coumarins from the fruits of Cnidium monnieri on leukemia cell lines. Planta Med. 2003;69(12):1091–5.
21. Chou SY, et al. Antitumor effects of Osthol from Cnidium monnieri: an in 71 vitro and in vivo study. Phytother Res. 2007;21(3):226–30.

22. Yang D, et al. Effects of osthole on migration and invasion in breast cancer cells. Biosci Biotechnol Biochem. 2010;74(7):1430–4.
23. Fujioka T, et al. Antiproliferative constituents from umbelliferae plants. V. A new furanocoumarin and falcarindiol furanocoumarin ethers from the root of Angelica japonica. Chem Pharm Bull (Tokyo). 1999;47(1):96–100.
24. Lin VC, et al. Osthole suppresses fatty acid synthase expression in HER2-overexpressing breast cancer cells through modulating Akt/mTOR pathway. J Agric Food Chem. 2010;58(8):4786–93.
25. Hung CM, et al. Osthole suppresses hepatocyte growth factor (HGF)-induced epithelial-mesenchymal transition via repression of the c-Met/Akt/mTOR pathway in human breast cancer cells. J Agric Food Chem. 2011;72 59(17):9683–90.
26. Nakamura T, et al. Inhibitory effect of oxycoumarins isolated from the Thai medicinal plant Clausena guillauminii on the inflammation mediators, iNOS, TNF-alpha, and COX-2 expression in mouse macrophage RAW 264.7. J Nat Med. 2009;63(1):21–7.
27. Qin LP, Wang HB, Zhang JQ. Effects of osthol and total-coumarins from Cnidium monnieri on immunological function in kidney yang deficiency mice. Zhongguo Zhong Xi Yi Jie He Za Zhi. 1995;15(9):547–9.
28. Terabe M, Berzofsky JA. Immunoregulatory T cells in tumor immunity. Curr Opin Immunol. 2004;16(2):157–62.
29. Reiter I, Krammer B, Schwamberger G. Cutting edge: differential effect of apoptotic versus necrotic tumor cells on macrophage antitumor activities. J Immunol. 1999;163(4):1730–2.
30. Wang P, et al. Betulinic acid exerts immunoregulation and anti-tumor effect on cervical carcinoma (U14) tumor-bearing mice. Pharmazie. 2012;67(8):733–9.
31. Biddle A, et al. CD44 Staining of Cancer Stem-Like Cells Is Influenced by Down-Regulation of CD44 Variant Isoforms and Up-Regulation of the Standard CD44 Isoform in the Population of Cells That Have Undergone 77 Epithelial-to-Mesenchymal Transition. PLoS ONE. 2013;8(2):e57314.
32. Piccirillo CA, Shevach EM. Naturally-occurring CD4 + CD25+ immunoregulatory T cells: central players in the arena of peripheral tolerance. Semin Immunol. 2004;16(2):81–8.
33. Sakaguchi S, et al. Immunologic self-tolerance maintained by activated T cells expressing IL-2 receptor alpha-chains (CD25). Breakdown of a single mechanism of self-tolerance causes various autoimmune diseases. J Immunol. 1995;155(3):1151–64.
34. Read S, Malmstrom V, Powrie F. Cytotoxic T lymphocyte-associated antigen 4 plays an essential role in the function of CD25(+)CD4(+) regulatory cells that control intestinal inflammation. J Exp Med. 2000;192(2):295–302.
35. Vojdani A, Erde J, Regulatory T. cells, a potent immunoregulatory target for CAM researchers: modulating tumor immunity, autoimmunity and alloreactive immunity (III). Evid Based Complement Alternat Med. 2006;3(3):309–16.
36. Shen X, et al. Increased prevalence of regulatory T cells in the tumor microenvironment and its correlation with TNM stage of hepatocellular carcinoma. J Cancer Res Clin Oncol.

2010;136(11):1745–54.
37. Waldmann TA, Dubois S, Tagaya Y. Contrasting roles of IL-2 and IL-15 in the life and death of lymphocytes: implications for immunotherapy. Immunity. 2001;14(2):105–10.
38. Fehniger TA, Cooper MA, Caligiuri MA. Interleukin-2 and interleukin-15: immunotherapy for cancer. Cytokine Growth Factor Rev. 2002;13(2):169–83.
39. Kwong B et al. Localized Immunotherapy via Liposome-Anchored Anti-CD137 + IL-2 Prevents Lethal Toxicity and Elicits Local and Systemic Antitumor Immunity. Cancer Res, 2013.
40. Wang Y, et al. SLUG is activated by nuclear factor kappa B and confers human alveolar epithelial A549 cells resistance to tumor necrosis factor-alpha-induced apoptosis. World J Surg Oncol. 2013;11:12.
41. Zhang W, et al. Tumour necrosis factor-alpha (TNF-alpha) transgene-expressing dendritic cells (DCs) undergo augmented cellular maturation and induce more robust T-cell activation and anti-tumour immunity than DCs generated in recombinant TNF-alpha. Immunology. 2003;108(2):177–88.
42. Zhang L, et al. Proteomic analysis of macrophages: a potential way to identify novel proteins associated with activation of macrophages for tumor cell killing. Cell Mol Immunol. 2007;4(5):359–67.
43. Tai DI, et al. Constitutive activation of nuclear factor kappaB in hepatocellular carcinoma. Cancer. 2000;89(11):2274–81.
44. Williams DH, et al. Protein kinase C is not a downstream effector of p21ras in activated T cells. Eur J Immunol. 1995;25(1):42–7.
45. Gomez J, et al. Role of NF-kappaB in the control of apoptotic and proliferative responses in IL-2-responsive T cells. Front Biosci. 1997;2:d49–60.
46. Nakatsuka K, et al. Purification of antigenic peptide from murine hepatoma cells recognized by Class-I major histocompatibility complex molecule-restricted cytotoxic T-lymphocytes induced with B7-1-gene-transfected hepatoma cells. J Hepatol. 1999;30(6):1119–29.
47. Kroger A, et al. Growth suppression of the hepatocellular carcinoma cell line Hepa1-6 by an activatable interferon regulatory factor-1 in mice. Cancer Res. 2001;61(6):2609–17.

Figures

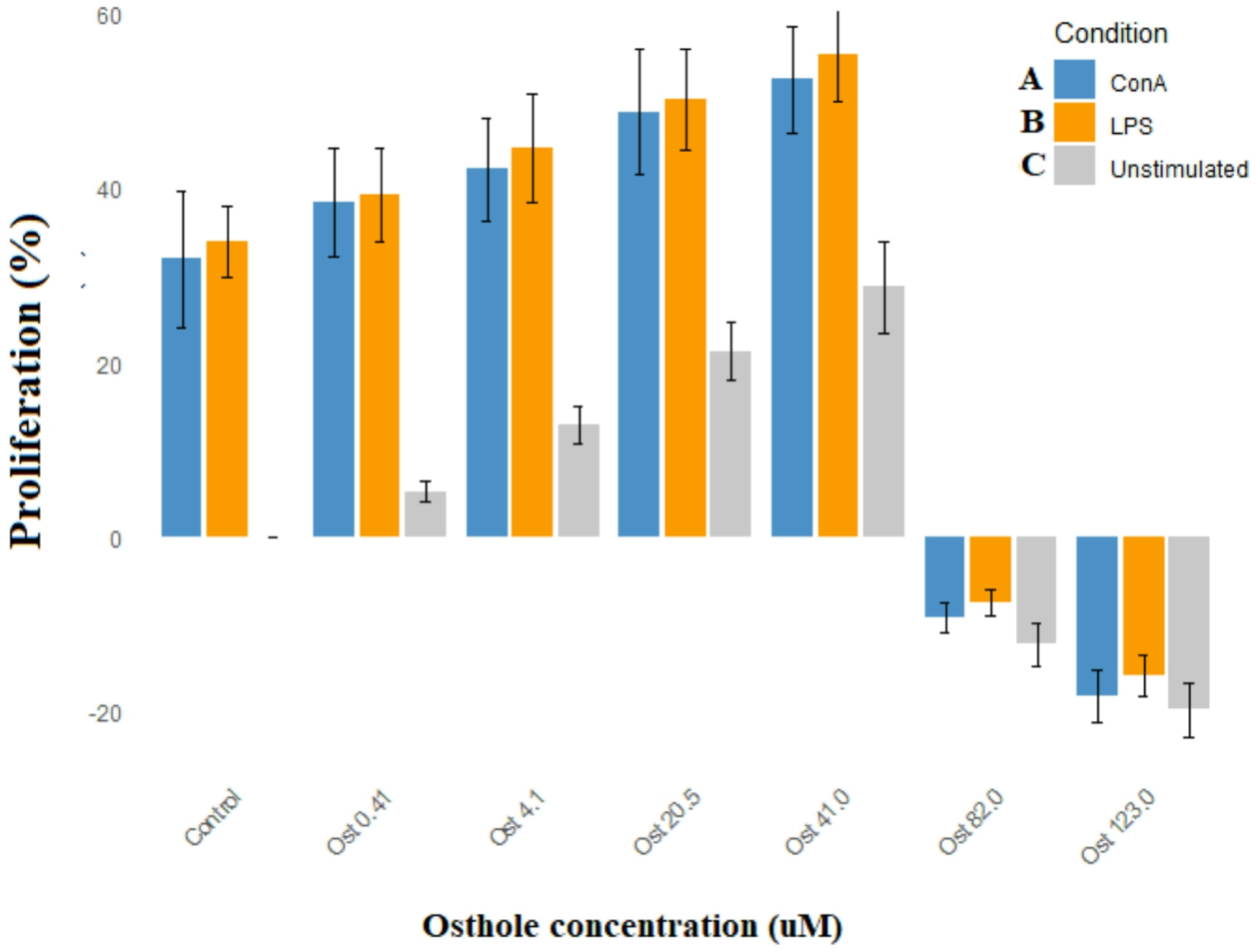


Figure 1

Osthole promotes splenocyte proliferation at low concentrations. Splenocytes from normal C57BL/6 mice were treated with indicated concentrations of osthole (μM) for 24 h, either unstimulated (**A**), stimulated with ConA (5 μg/mL, (**B**), LPS (3 μg/mL, (**C**). Proliferation rate (%) = (OD treated/OD control – 1) × 100%. Data are mean ± SD (n=3). *$p < 0.05$, **$p < 0.01$ vs. control (unstimulated) or vs. mitogen alone (ConA, LPS). Note: Negative values indicate inhibition.

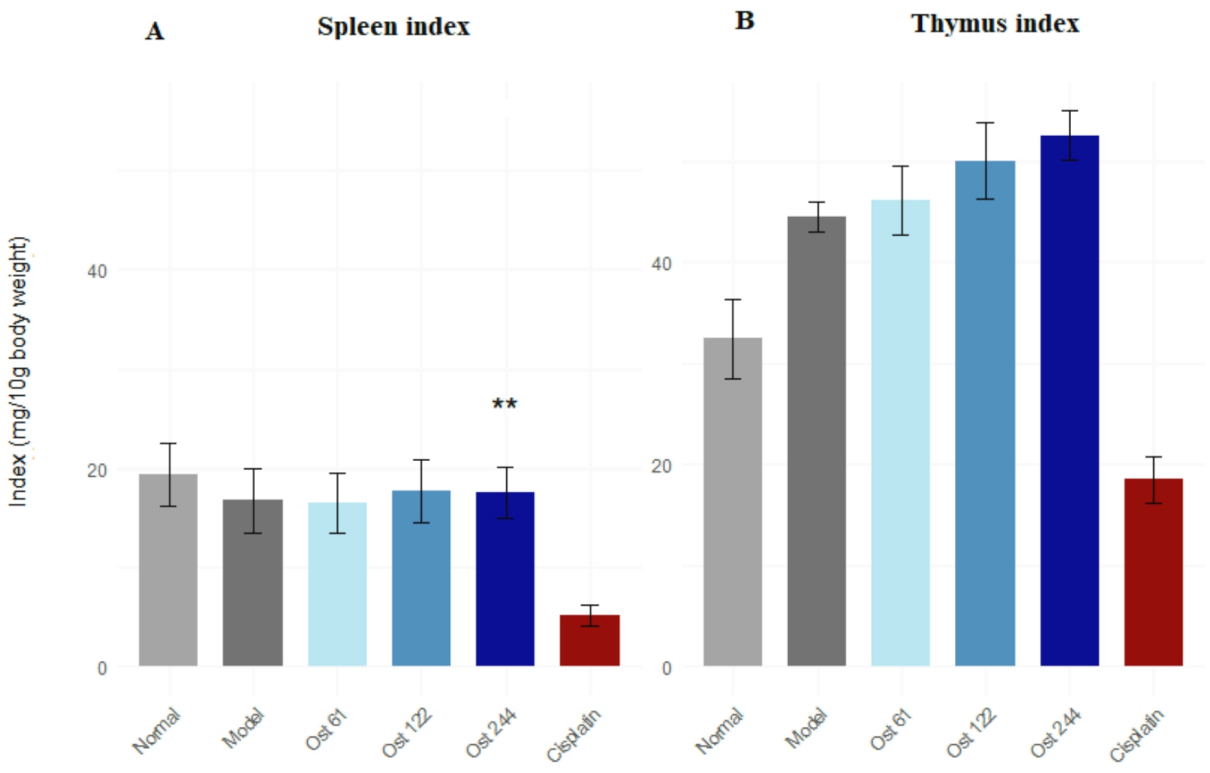


Figure 2

Effect of osthole on thymus and spleen indices in HCC-bearing mice. (**A**) Thymus index; (**B**) Spleen index. Indices = organ weight (mg) / body weight (g) × 10. Data are mean ± SD (n=5). ***p* < 0.01 vs. model control; ##*p* < 0.01 vs. normal control. Osthole doses are in mg/kg, i.p., daily for 14 days. Cisplatin: 5 mg/kg, i.p., every other day.

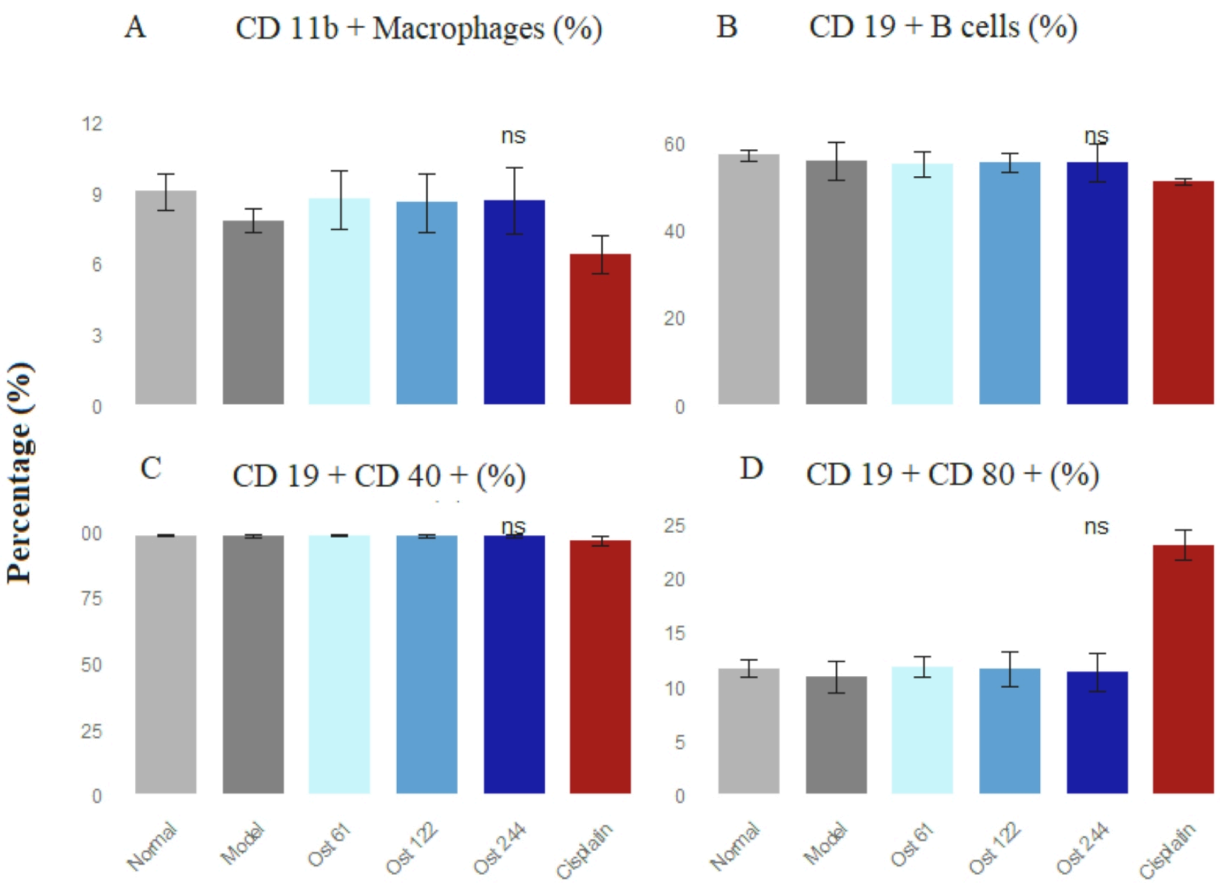


Figure 3

Osthole does not significantly alter B cell subsets or macrophage proportion in spleen. (**A**) $CD19^+$ B cells (%); (**B**) $CD19^+$ $CD80^+$ activated B cells (%); (**C**) $CD19^+$ $CD40^+$ mature B cells (%); (**D**) $CD11b^+$ macrophages (%). Data are mean ± SD (n=5). ns = not significant ($p > 0.05$ vs. model control). *$p < 0.05$ vs. normal control (for macrophages). Osthole doses: 61, 122, 244 mg/kg. Cisplatin: 5 mg/kg.

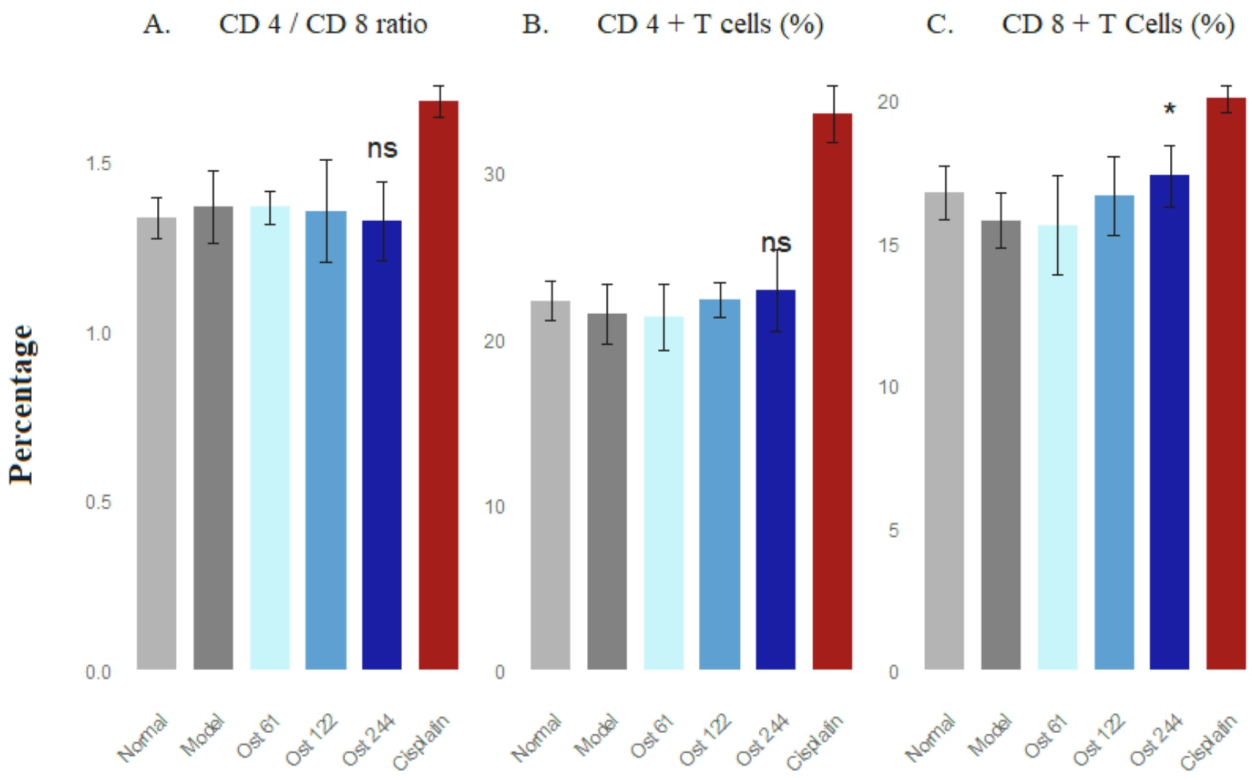


Figure 4

Osthole increases CD8⁺ T cell proportion and number without affecting CD4⁺ T cells or CD4/CD8 ratio. (**A**) CD4⁺ T cells (%); (**B**) CD8⁺ T cells (%); (**C**) CD4⁺/CD8⁺ ratio. Data are mean ± SD (n=5). *p < 0.05 vs. model control; ns = not significant. Osthole at 244 mg/kg significantly increased CD8⁺ T cell percentage. Absolute CD8⁺ T cell numbers were also significantly increased.

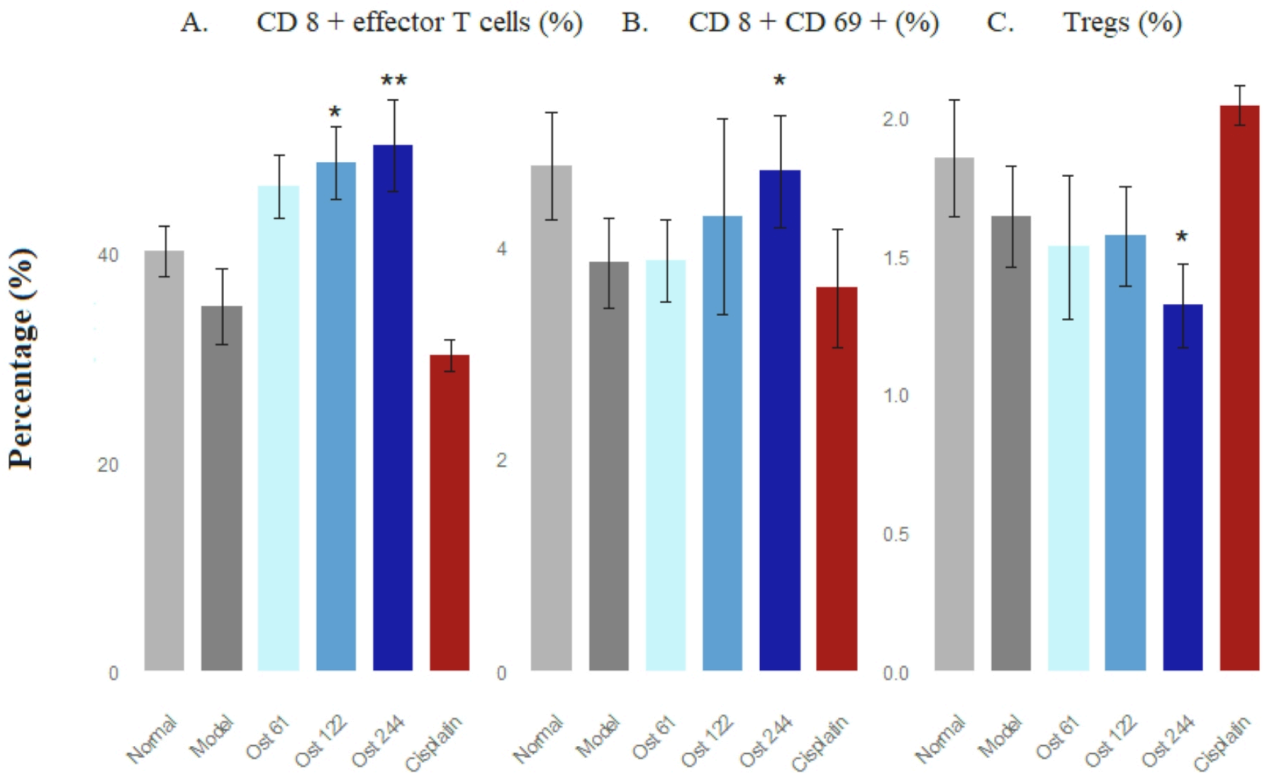


Figure 5

Osthole enhances CD8⁺ T cell activation, promotes effector differentiation, and reduces Tregs. (**A**) CD8⁺ CD69⁺ activated T cells (%); (**B**) CD8⁺CD44⁺CD62L⁻ effector T cells (%); (**C**) CD4⁺CD25⁺Foxp3⁺ regulatory T cells (%). Data are mean ± SD (n=5). *p < 0.05, **p < 0.01 vs. model control; ns = not significant. Osthole at 244 mg/kg restored CD8⁺ activation, dose-dependently increased effector CD8⁺ T cells, and reduced Tregs.

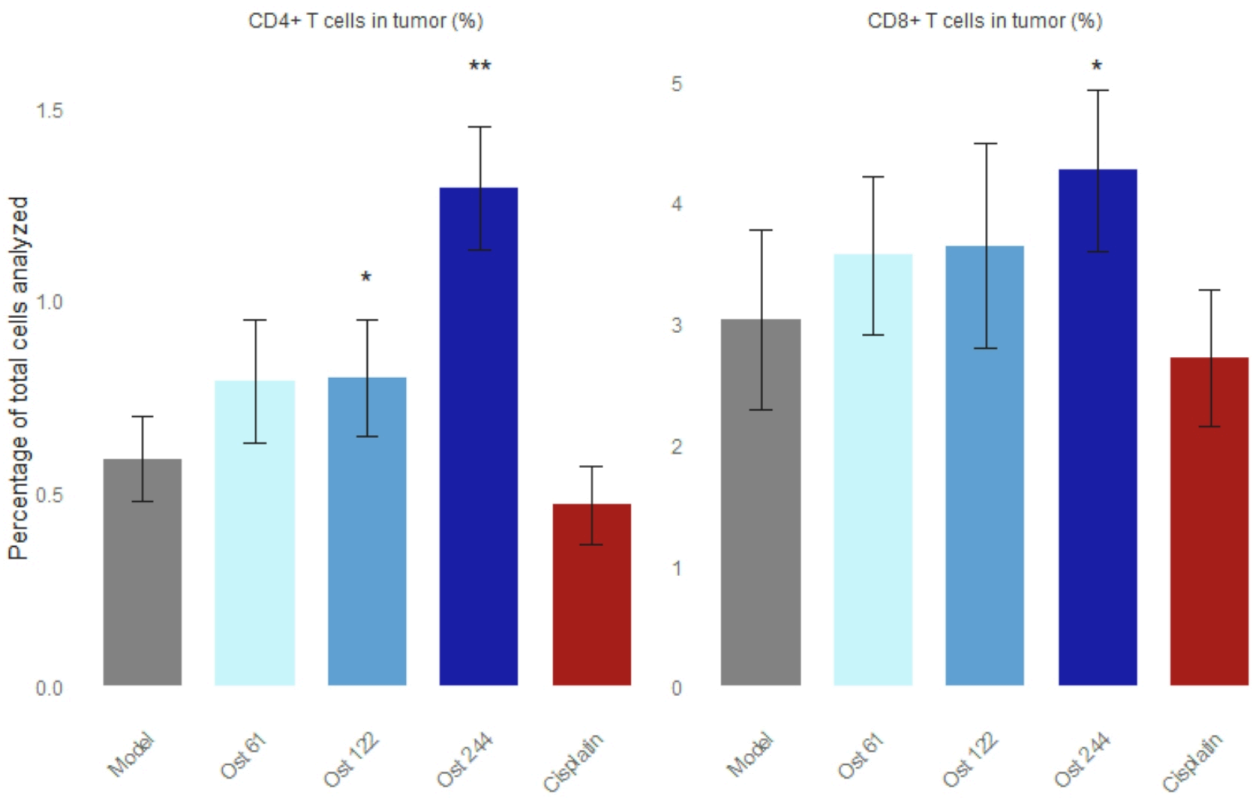


Figure 6

Osthole increases tumor-infiltrating CD4⁺ and CD8⁺ T cells. (A) CD4⁺ T cells in tumor (% of 10,000 cells); (B) CD8⁺ T cells in tumor (%). Data are mean ± SD (n=5). *p< 0.05, **p < 0.01 vs. model control. Osthole at 122 and 244 mg/kg significantly increased CD4⁺ infiltration, and at 244 mg/kg increased CD8⁺ infiltration. Cisplatin had no effect.

Supplementary Files

This is a list of supplementary files associated with this preprint. Click to download.

- Onlinefloatimage1.png